Metamagnetic transition and the anomalous virgin magnetization curve in $Ce(Fe_{0.96}Ru_{0.04})_2$

2008 J. Phys.: Condens. Matter 20 025209

(http://iopscience.iop.org/0953-8984/20/2/025209)

J. Phys.: Condens. Matter **20** (2008) 025209 (6pp) doi:10.1088/0953-8984/20/02/025209

Metamagnetic transition and the anomalous virgin magnetization curve in $Ce(Fe_{0.96}Ru_{0.04})_2$

M K Chattopadhyay and S B Roy

Magnetic and Superconducting Materials Section, Raja Ramanna Centre for Advanced Technology, Indore 452013, India

Received 9 August 2007, in final form 24 October 2007
Published 6 December 2007
Online at stacks.iop.org/JPhysCM/20/025209

Abstract

We present results of dc magnetization measurements investigating the magnetic field-induced metamagnetic transition in $Ce(Fe_{0.96}Ru_{0.04})_2$. In the temperature region where this material undergoes a ferromagnetic to antiferromagnetic first-order phase transition, the isothermal virgin magnetization curve lies distinctly outside the envelope magnetization curve obtained in the subsequent field cycles. We show that this anomalous behaviour of the virgin magnetization curve arises due to the dependence of the initial zero field magnetic state on the temperature–field history of the sample in the concerned temperature regime. This origin of the anomalous virgin magnetization curve is distinctly different from the very similar behaviour observed earlier in Al- and Os-doped $CeFe_2$ alloys, where this feature was associated with the kinetic arrest of the first-order ferromagnetic to antiferromagnetic transition.

(Some figures in this article are in colour only in the electronic version)

1. Introduction

$CeFe_2$ is a cubic Laves phase ferromagnet (with $T_{Curie} \approx 230$ K) [1] where small substitution (<10%) of selected elements such as Co, Al, Ru, Ir, Os and Re can induce a low temperature antiferromagnetic state [2, 3]. In recent years we have studied in some detail the magnetic field-induced transition from antiferromagnetic (AFM) to ferromagnetic (FM) state (or the metamagnetic transition [4]) in various Al and Ru-doped alloys [5–7]. One of the interesting findings of these studies is an anomalous feature associated with the isothermal virgin magnetization (M) versus magnetic field (H) curves in Al-doped $CeFe_2$ alloys [5]. This feature arises in the form of the virgin M–H curve lying distinctly outside and below the envelope M–H curve obtained in the subsequent field cycles. This anomalous behaviour was attributed to the kinetic arrest of the reverse transition from the FM to AFM state in the field decreasing cycle [5]. Later on such anomalous behaviour of the virgin M–H curve has been observed in various other classes of magnetic systems like manganese oxide compounds showing colossal magnetoresistance (CMR) [8, 9], $Mn_2Sb_{0.95}Sn_{0.05}$ [10], RhFe [11] and Nd_7Rh_3 [12] and magnetocaloric material Gd_5Ge_4 [13]. Here taking the example of a $Ce(Fe_{0.96}Ru_{0.04})_2$ alloy, we show that this anomalous feature of the virgin M–H curve lying outside the envelope M–H curve can also arise in a relatively narrow temperature regime around the FM–AFM transition temperature, without being actually related to a process of kinetic arrest of this phase transition. We shall discuss the origin of this anomalous behaviour, and also how this differs from the one associated with the kinetic arrest of the reverse metamagnetic transition.

2. Experimental details

The $Ce(Fe_{0.96}Ru_{0.04})_2$ polycrystalline alloy used in the present study was prepared by argon-arc melting. The details of the sample preparation and characterization have been described earlier [2, 3]. Neutron diffraction studies of the same sample revealed a discontinuous change of the unit cell volume at the FM–AFM transition, confirming that it is first-order [3]. Bulk magnetization measurements were made with a commercial vibrating sample magnetometer (VSM; Quantum Design).

3. Results and discussion

Figure 1 shows the isothermal magnetization (M) versus field (H) plot for $Ce(Fe_{0.96}Ru_{0.04})_2$ at 5 K. The virgin M–H curve

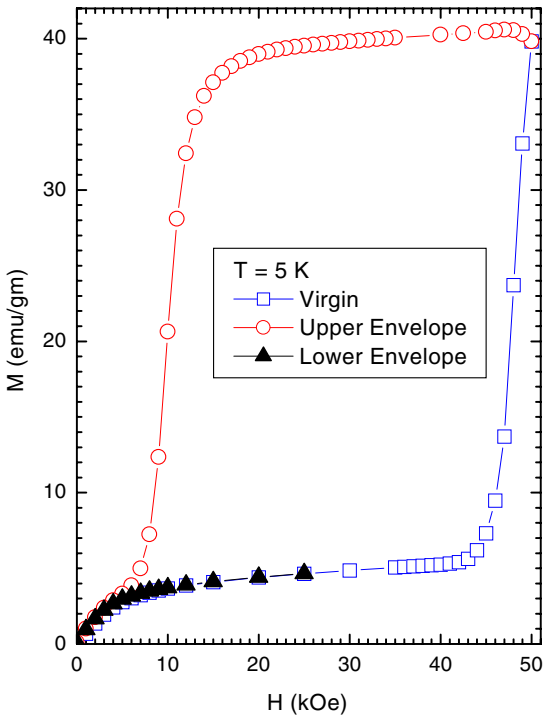

Figure 1. Isothermal magnetization (M) versus field (H) plot for $Ce(Fe_{0.96}Ru_{0.04})_2$ at $T = 5$ K. The virgin magnetization curve coincides with the lower envelope curve. All the data points for the lower envelope are not shown in the figure for clarity of the presentation. Also for the sake of clarity and conciseness we present the M–H curve in the first quadrant only. Inclusion of the data for the negative values of H would produce a symmetrical M–H loop in the third quadrant.

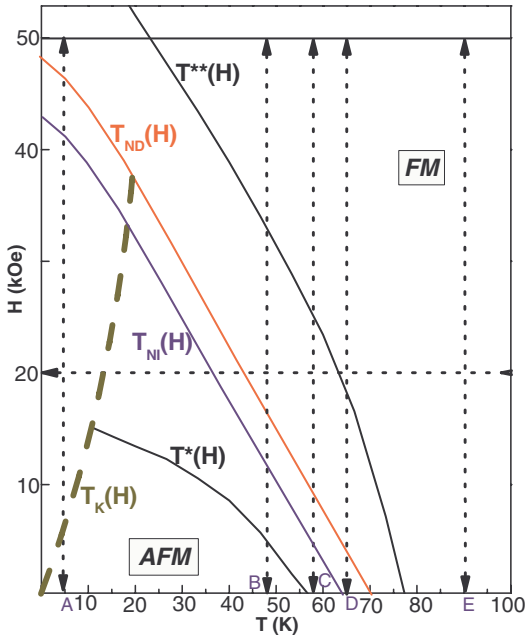

Figure 2. Schematic phase diagram of $Ce(Fe_{0.96}Ru_{0.04})_2$ showing FM–AFM transition lines ($T_{NI}(H)$, $T_{ND}(H)$), limits of superheating ($T^{**}(H)$) and supercooling ($T^{*}(H)$), and the line of kinetic arrest ($T_K(H)$). See text for details. The dotted vertical lines with arrowheads show the path traversed in the phase space during isothermal M–H experiments (see text for details). The dashed horizontal line with arrowhead gives the example of an FCC (field cooled cooling) path.

was initiated from a zero field cooled (ZFC) state prepared by cooling the sample in zero field from 250 K (which is well above the AFM to FM transition temperature) to 5 K, and then increasing H to 50 kOe. Measurement of M was then continued with the cycling of H between 50 and -50 kOe. The M–H curve thus obtained is called the envelope curve. This third leg of the M–H cycle between -50 and 50 kOe is called the lower envelope curve, and the virgin M–H curve is found to coincide with this curve.

In our earlier temperature dependent magnetization study on the same alloy system, it was shown that when the applied H is greater than 15 kOe the first-order FM–AFM transition process was kinetically arrested in the temperature regime $T < 23$ K [14]. Following the arguments in [5], the virgin M–H curve in the isothermal M–H measurements is expected to lie outside the envelope M–H curve due to the kinetic arrest of the FM to AFM transition. To understand this apparent contradiction in the results of isothermal M–H studies at $T = 5$ K (see figure 1), we examine carefully the schematic phase diagram of $Ce(Fe_{0.96}Ru_{0.04})_2$ presented in figure 2. This phase diagram is formed on the basis of our earlier experimental results [6, 7, 15, 16]. In figure 2, the $T^{*}(H)$ and $T^{**}(H)$ curves represent respectively the limits of supercooling and superheating [4] across the transition. These are end points of the FM–AFM transition in the decreasing and increasing temperature and field cycles respectively, and are marked by the limits of thermal and field hysteresis in an observable (namely, magnetization or electrical resistance) with varying T and H [6, 7, 15, 16]. The entire sample is in the equilibrium FM state for $T > T^{**}(H)$. Below $T^{*}(H)$, the whole sample is in the equilibrium AFM state. We have explained in our earlier works [6, 15] that due to quenched disorder there is a landscape of transition temperatures (T_N) in these materials. This is in line with the theoretical works of Imry and Wortis [17]. The curve $T_{NI}(H)$ in figure 2 denotes the onset of the AFM to FM transition and could be identified from a sharp rise in M with increasing T in the M–T curves measured in constant field. Since the AFM–FM transition could be driven by H as well, the same onset of transition could be determined from a sharp rise in M with increasing H on the isothermal M–H curves. The criterion for the determination of the onset of the transition has been explained in [6]. The curve $T_{ND}(H)$ in figure 2 denotes the onset of the FM to AFM transition that could be brought about both by decreasing T and H. Note that $T_{NI}(H)$ and $T_{ND}(H)$ respectively are distinct from the limits of metastability $T^{**}(H)$ and $T^{*}(H)$ of the first-order phase transition. It is to be noted that for $Ce(Fe_{0.96}Ru_{0.04})_2$ $T_{ND}(H) > T_{NI}(H)$, and this is explained with the help of the rough landscape picture of the transition onsets [6, 14]. Co-existence of the AFM and FM phases could be observed in the regime $T^{*}(H) < T < T_{ND}(H)$ while cooling, and $T_{NI}(H) < T < T^{**}(H)$ while heating. The $T_K(H)$ line (thick dashes) marks the regime where the FM to AFM first-order transition process is arrested/hindered. It is worthwhile to note that T_K does not represent any sharp

cut-off or boundary. It may also be noted that $T_K(H)$ loses significance in the regime above $T_{ND}(H)$ in the H–T phase space since the FM to AFM transition does not take place here. On the other hand the limit of supercooling $T^*(H)$ can be obtained experimentally only if $T^*(H)$ is reached before crossing the $T_K(H)$ line. This definitely happens during the FCC (field cooled cooling) experiments (when the sample is cooled from $T > T^{**}(H)$ down to a relevant temperature in the presence of a constant magnetic field) for $H < 15$ kOe [7]. The sample then reaches a stable AFM phase below T^*, and no kinetic arrest is observed on this FCC path. But for larger H values, on a FCC path $T_K(H)$ is reached before $T^*(H)$. In figure 2, the dotted horizontal line at $H = 20$ kOe with an arrowhead is an example of such an FCC path. Once the kinetic arrest sets in, the limit of supercooling is never reached on further lowering of T. Thus the $T^*(H)$ line is not drawn below the temperatures $T < T_K(H)$. However, if the state of kinetic arrest is attained through a high field FCC path, the $T_K(H)$ line can be reached experimentally by decreasing H isothermally. We would like to note here that figure 2 is a schematic diagram, and the lines do not represent exact values of T and H. The disorder-broadened nature of the FM–AFM transition, and the slowness of dynamics of the kinetic arrest renders the experimental determination of $T_K(H)$ and the onsets and limits of the FM–AFM transition rather difficult. The points A, B, C, D, and E on the T-axis of figure 2 represent the temperatures at which the isothermal M–H measurements (to be described) are performed. The double headed arrows (along with the dotted vertical lines) at points A, B, C, etc represent the path traversed in the H–T phase space during the isothermal M–H measurements. The horizontal line at $H = 50$ kOe represents the field limit for the present experiments.

We now analyse the results of isothermal M–H measurements at $T = 5$ K (figure 1) with the help of the phase diagram of $Ce(Fe_{0.96}Ru_{0.04})_2$ shown in figure 2. The point A in figure 2 represents $T = 5$ K and $H = 0$. The sample is in the equilibrium AFM state. As H is increased (moving upwards along the dotted vertical line starting from the point A of figure 2) the AFM to FM transition sets in once the $T_{NI}(H)$ line is crossed. This transition is marked by an abrupt rise in M (see figure 1). The H-decreasing experiment is initiated before the limit of superheating is reached. The AFM fraction in the sample remains metastable at the point (5 K, 50 kOe), and the field reversal acts as a disturbance or fluctuation that converts a portion of the metastable (AFM) phase to the stable (FM) phase [6]. This causes a rise of M upon field reversal (figure 1). As H is decreased we move downwards along the dotted vertical line at A. When the $T_{ND}(H)$ line is crossed with decreasing H, the FM phase is supercooled but the FM to AFM transition is kinetically arrested. That the FM phase is arrested and glass-like is confirmed through magnetic relaxation experiments as well [18]. Lowering of H further causes a gradual de-arrest of the FM fraction, though the temperature is not increased. The FM to AFM transition is completed as H is decreased so as to cross the $T_K(H)$ line. This sequence remains unchanged when H is negative, and hence a symmetric M–H loop is obtained in the third quadrant

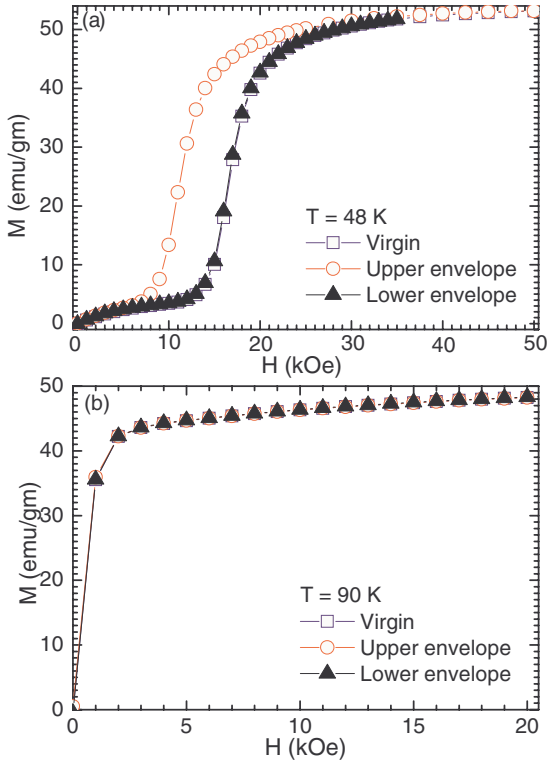

Figure 3. Isothermal magnetization (M) versus field (H) plots for $Ce(Fe_{0.96}Ru_{0.04})_2$ at (a) $T = 48$ K and (b) $T = 90$ K.

(not shown here for clarity and conciseness). After this field cycling, the magnetic state in the sample remains the same as in the virgin state and on increasing the field again from zero, the lower envelope curve coincides with the virgin M–H curve. This behaviour is in sharp contrast with the isothermal field dependence of M in $Ce(Fe_{0.96}Al_{0.04})_2$ at $T = 5$ K, where the virgin M–H curve was found to lie outside the envelope curves [5]. This latter behaviour was attributed to the kinetic arrest of the first-order field-induced FM to AFM transition [5]. This qualitative difference in the M–H behaviour at $T = 5$ K originates from the difference in the H dependence of T_K for $Ce(Fe_{0.96}Ru_{0.04})_2$ and $Ce(Fe_{0.96}Al_{0.04})_2$ alloys. The difference is clearly seen through the comparison of figure 3(c) of [5] and figure 2 of the present paper. In the case of $Ce(Fe_{0.96}Al_{0.04})_2$ at 5 K, some part of the sample still remains in the kinetically arrested state after reducing the field to zero from the high field FM state. So in the subsequent field increasing cycle the sample magnetization in the low field regime will be higher than that in the virgin M–H curve initiated from the zero field cooled state.

In figures 3 and 4 we present results of isothermal M–H measurements in $Ce(Fe_{0.96}Ru_{0.04})_2$ for $T = 48$, 58, 60, 62, 65, and 90 K. For these experiments, the target temperature (say 48 K) was reached by cooling the sample down to 30 K (in the ZFC protocol) first, followed by warming the sample up to this target temperature in zero field. The reason for choosing this experimental protocol for preparing the ZFC state for the isothermal M–H measurements will become clear later on. We summarize below the results of these isothermal M–H measurements.

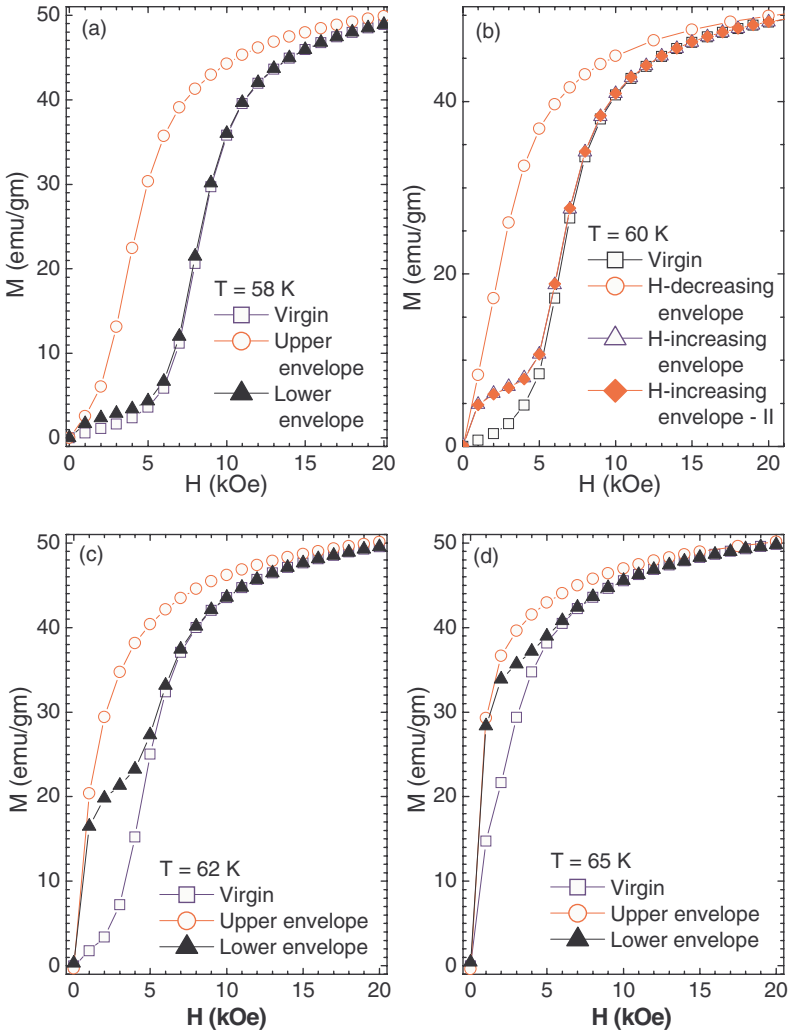

Figure 4. Isothermal magnetization (M) versus field (H) plots for $Ce(Fe_{0.96}Ru_{0.04})_2$ at $T = 58$, 60, 62, and 65 K showing the change of the shape of the virgin and the envelope magnetization curves with increasing temperature. While these M–H curves are drawn up to a maximum field of 50 kOe, the higher field (>20 kOe) M–H data are not shown here for the sake of clarity and conciseness. For figure (b), a second H-increasing envelope M–H curve is recorded after two full H-cycles between 50 and −50 kOe.

(1) The area enclosed by the upper and the lower envelope M–H curves decreases with rising T.
(2) The virgin M–H curve coincides with the lower envelope M–H curve for $T \leqslant 56$ K.
(3) For $T \geqslant 77$ K, virgin, upper, and lower envelope M–H curves all overlap.
(4) The virgin M–H curve lies outside the envelope M–H curves for 56 K $< T <$ 77 K.
(5) The shape and size of the area enclosed by the lower envelope curve and the virgin M–H curve change systematically with increasing T.

We now analyse these results with the help of the H–T phase diagram shown in figure 2. At $T = 48$ K, as H is increased from zero during the M–H experiments, one moves upward along the vertical line drawn from B in figure 2. The AFM to FM transition sets in when this vertical line intersects the $T_{NI}(H)$ line, and this is marked by a sharp rise in M in the virgin curve (see figure 3(a)). Similarly, in the decreasing H cycle the FM to AFM transition takes place when the vertical line towards B intersects the $T_{ND}(H)$ line. The limits of metastability are the points where the vertical line intersects the $T^{**}(H)$ line and $T^{*}(H)$ line. While initiating the M–H experiments, the point B (see figure 2) is reached after warming from 30 K in zero field. For $H = 0$, 30 K is well below T^{*}. This ensures that on reaching the point B (after ZFC) the sample is entirely in the AFM state, i.e. there is no supercooled FM fraction in the sample. On reaching point B in the H-decreasing cycle (i.e. following the upper envelope curve), the sample is once again entirely in the AFM state. The lower envelope M–H curve obtained in the subsequent H-increasing cycle, would then clearly coincide with the virgin M–H curve. Such behaviour of M–H curves provides a typical example of the isothermal response of $Ce(Fe_{0.96}Ru_{0.04})_2$ applied to magnetic fields in the temperature regime $T \leqslant 56$ K.

Above 77 K the sample is entirely in the FM state (see figure 3(b)) and is represented by the point E in figure 2. The M–H curve at $T = 90$ K (see figure 2) is like that of a soft ferromagnet. It is worthwhile to mention here that undoped

$CeFe_2$ is known to be a soft ferromagnet that exhibits no field history effects [19].

Warming up from the ZFC state at 30 K to point C ($T = 58$ K) in figure 2 does not cause any phase transition from the AFM state to the FM state in the sample as the $T_{NI}(H)$ line is not crossed; the sample still remains in the AFM state. With the increase in H isothermally, the AFM to FM transition, however, is clearly visible in the virgin M–H curve (see figure 4(a)). But the return transition from the FM to AFM state is not completed on decreasing the field to zero as the point C (see figure 2) is above $T^*(H)$ at $H = 0$ and $T = 58$ K. Hence at $H = 0$, a fraction of the sample remains in the supercooled FM state. Now if H is increased from zero again, the measured M represents the response of a configuration with both stable AFM and metastable FM fractions. And because of this FM fraction, the lower envelope M–H curve lies above the virgin M–H curve (see figure 4(a)). The situation is similar for $T = 60$ and 62 K, and accordingly the virgin M–H curve lies outside the envelope curves for these temperatures as well (see figures 4(b) and (c)). The length of the intercept of a vertical line between $T_{ND}(H)$ and the T-axis (figure 2) is proportional to the fraction of FM phase that is transformed to the AFM state while decreasing H (for the points C and D). The higher the temperature at C, the shorter is this intercept, and the larger is the remaining metastable FM fraction, and therefore the higher is the position of the lower envelope M–H curve above the virgin curve. The remaining metastable FM fraction is not affected by further H-cycling in either sign of H. This is shown in figure 4(b) for $T = 60$ K. A second H-increasing envelope M–H curve recorded after two full H-cycles between 50 and −50 kOe, re-traces completely the first H-increasing envelope M–H curve. The virgin M–H curve cannot be recovered unless the initial ZFC state is freshly prepared.

The point D in figure 2 represents the point ($T = 65$ K, $H = 0$) and it is above $T_{NI}(H)$. As the sample is warmed up to this point from $T = 30$ K, a significant portion of the sample is already in the FM phase at $H = 0$. The remaining sample would be in the superheated AFM state. Increasing H isothermally would effectively decrease the energy barrier separating the AFM and FM states. So, there would be further AFM to FM transformation. Since the virgin M–H curve for $T = 65$ K (see figure 4(d)) represents M for a configuration consisting of the FM fraction along with a co-existing metastable AFM phase, the shape of the virgin M–H curve at 65 K is qualitatively different from those at the lower T values. While decreasing H, only a very small fraction of the FM phase is converted to the AFM phase. Also now at $H = 0$, the superheated AFM fraction present in the initial ZFC state will be absent; it is converted into the stable FM state due to the energy fluctuations introduced during the magnetic field cycling. Thus the lower envelope M–H curve represents a larger FM fraction in the sample than the virgin M–H curve, and consequently the M values of the lower envelope M–H curve are higher.

This striking feature of the virgin M–H curve in $Ce(Fe_{0.96}Al_{0.04})_2$ was earlier rationalized in terms of the kinetic arrest of a first-order phase transition [5]. In contrast, the present

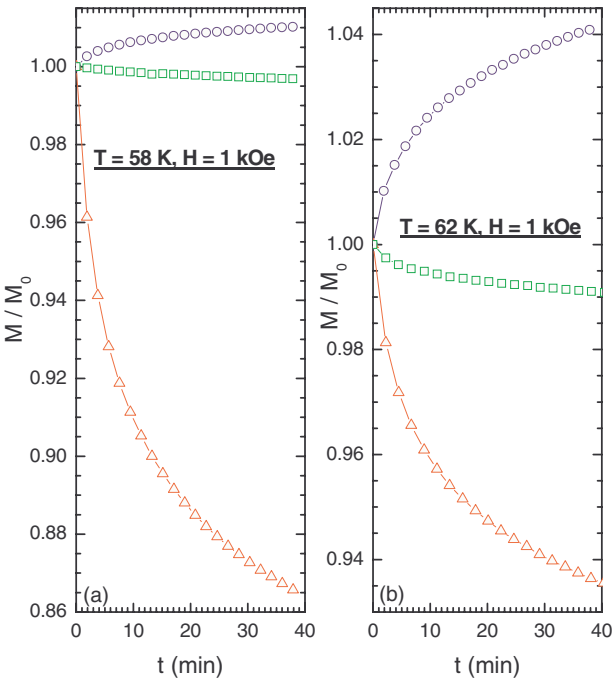

Figure 5. Normalized magnetization versus time (relaxation) graphs for $Ce(Fe_{0.96}Ru_{0.04})_2$ obtained at constant magnetic field (1 kOe) and temperature ((a) 58 K and (b) 62 K). Symbols: open circles depict the magnetic relaxation on the virgin curve; open triangles and open squares respectively depict the magnetic relaxation on the upper and lower envelope magnetization curves. M_0 denotes the M value recorded just after reaching the target field value of 1 kOe.

phenomenon of the virgin M–H curve lying outside the envelope M–H curves in $Ce(Fe_{0.96}Ru_{0.04})_2$, is explained in terms of the standard phenomenology of a first-order phase transition, namely, metastability and phase co-existence [4], and without involving the concept of kinetic arrest of the first-order FM–AFM phase transition. In the analysis of the isothermal M–H curves of $Ce(Fe_{0.96}Ru_{0.04})_2$ (figures 1, 3 and 4), we find that within the T-regime where the anomalous behaviour of the isothermal virgin M–H curve is observed, the phenomenon becomes more prominent initially with increasing T before vanishing ultimately in the FM regime. In contrast, had this phenomenon of the virgin M–H curve lying outside the envelope M–H curves been due to the kinetic arrest of the first-order phase transformation, as it was in the case of $Ce(Fe_{0.96}Al_{0.04})_2$ alloy, the magnitude of the anomaly would have increased with the lowering in T [5]. This opposite temperature dependence of the anomalous behaviour of the isothermal virgin M–H curve enables us to discern clearly its physical origin.

We shall now present the results of magnetization relaxation measurements to support the conjecture that the phenomenon of the virgin M–H curve lying outside the envelope M–H curves in $Ce(Fe_{0.96}Ru_{0.04})_2$ is not related to the kinetic arrest of the first-order AFM–FM phase transition. Figure 5 shows the results of M versus time plots at $T = 58$ K and $T = 62$ K on the virgin, upper, and lower envelope magnetization curves at $H = 1$ kOe (see the figure caption for details). Here, the temperatures 58 and 62 K were reached using the same experimental protocol as for the isothermal M–

H experiments. For both T values, we observe that M relaxes with time towards a higher value on the virgin magnetization curve; while on the upper and lower envelope curves, M relax to attain lower values. These relaxation results could be analysed with the help of the phase diagram of figure 2. At 58 and 62 K, the sample is entirely in the AFM state at $H = 0$ (below $T_{NI}(H)$). We again recall that in $Ce(Fe_{0.96}Ru_{0.04})_2$ we are dealing with a disorder-broadened first-order FM–AFM phase transition having a spatial distribution of the transition-temperatures over the sample. Under such a situation the $T_{NI}(H)$ line of figure 2 actually broadens to become a quasi-continuous band and the exact experimental determination of $T_{NI}(H)$ becomes difficult [6]. As H is raised to 1 kOe from the ZFC state, a portion of the sample possibly crosses the $T_{NI}(H)$ line locally. As a result, a fraction of the AFM phase becomes metastable [6] which gives rise to relaxation in M. Because of AFM (metastable state) to FM (stable state) conversion, M increases with time. It is easy to understand from the schematic diagram (figure 2) that the barrier height separating the metastable and stable phases is smaller at the higher temperature of 62 K. Hence the $H = 1$ kOe point on the virgin curve for $T = 62$ K registers a larger degree of relaxation (compare figures 5(a) and (b)). On the upper envelope curve, both for $T = 58$ K and 62 K, at $H = 1$ kOe the sample is well below $T_{ND}(H)$ but is above the $T^*(H)$ line. The FM phase is metastable in this case, and it goes to the stable AFM phase with time. This produces a relaxation in M towards lower values. We have argued earlier that on the upper envelope curve, at $H = 0$, a fraction of the supercooled FM phase is retained. As the field is now increased, the reversal of the direction of the field change probably causes energy fluctuations in the supercooled phase, which then gets converted to the AFM phase. But in other portions of the sample, at $H = 1$ kOe, a fraction of the AFM phase becomes metastable, as explained in connection with the relaxation results on the virgin curve. In this picture, the sample goes to a very special state of phase co-existence where two different parts of the sample exhibit two different kinds of metastability. This gives rise to a competing process where the relaxation due to the supercooled FM fraction wins over that due to the superheated AFM fraction. Thus in our global measurement of M, we observe M to decrease slowly with time. At $T = 62$ K, a larger fraction of supercooled FM fraction is retained and accordingly a bigger degree of reduction of M with time is recorded on the lower envelope (compare figures 5(a) and (b)) at $H = 1$ kOe. None of the relaxation data presented in figure 5 could be fitted to the Kohlrausch–Williams–Watt (KWW) stretched exponential function, as was possible in the low T regime where the kinetic arrest of the FM–AFM transition led to a non-ergodic glass-like magnetic state [14].

In conclusion, we have studied in detail the isothermal field dependence of magnetization in $Ce(Fe_{0.96}Ru_{0.04})_2$. We find that in a temperature regime around the FM–AFM transition temperature of this alloy, the isothermal virgin M–H curve shows an anomalous behaviour, namely it resides outside the envelope M–H curve. Earlier, the same feature was observed in $Ce(Fe_{0.96}Al_{0.04})_2$ alloy [5] in the low temperature regime well below the FM–AFM transition temperature, and this was considered to be a signature of the kinetic arrest of the field-induced first-order FM–AFM transition. We have argued here that the shape of the $T_K(H)$ line in the H–T phase diagram can lead to such behaviour in the low temperature isothermal M–H curves in $Ce(Fe_{0.96}Al_{0.04})_2$, but not in $Ce(Fe_{0.96}Ru_{0.04})_2$. We have shown that in $Ce(Fe_{0.96}Ru_{0.04})_2$ the anomalous behaviour in the isothermal virgin M–H curve arises due to metastability associated with the first-order phase transition process itself, and not due to the kinetic arrest of the first-order phase transition process. The present work also highlights how the temperature dependence of the anomalous virgin M–H curve can be used to discern the origin of this behaviour. The important message here is that the existence of an anomalous behaviour in the isothermal virgin M–H curve alone is not enough to prove the presence of a low temperature magnetic-glass state [5]. Detailed studies of the field–temperature history dependence and the dynamical response of the system are necessary to reach a firm conclusion [14].

References

[1] Paolasini L *et al* 1998 *Phys. Rev.* B **58** 12117 and references therein
[2] Roy S B and Coles B R 1989 *J. Phys.: Condens. Matter* **1** 419
Roy S B and Coles B R 1990 *Phys. Rev.* B **39** 9360
[3] Kennedy S J and Coles B R 1990 *J. Phys.: Condens. Matter* **2** 1213
[4] Chaikin P M and Lubensky T C 1995 *Principles of Condensed Matter Physics* (Cambridge: Cambridge University Press)
[5] Manekar M A *et al* 2001 *Phys. Rev.* B **64** 104416
[6] Chattopadhyay M K *et al* 2003 *Phys. Rev.* B **68** 174404
[7] Sokhey K J S *et al* 2004 *Solid State Commun.* **129** 19
[8] Banerjee A *et al* 2006 *J. Phys.: Condens. Matter* **19** 256211
Rawat R *et al* 2007 *J. Phys.: Condens. Matter* **19** 256211
[9] Hur N H and Dho J 2003 *Phys. Rev.* B **67** 214414
[10] Jhang Y Q, Zhang Z D and Aarts J 2004 *Phys. Rev.* B **70** 132407
Jhang Y Q, Zhang Z D and Aarts J 2005 *Phys. Rev.* B **71** 229902(E)
[11] Maat S, Thiele J-U and Fullerton E E 2005 *Phys. Rev.* B **72** 214432
[12] Sengupta K and Sampathkumaran E V 2006 *Phys. Rev.* B **73** 020406(R)
[13] Tang H *et al* 2004 *Phys. Rev.* B **69** 064410
Chattopadhyay M K *et al* 2004 *Phys. Rev.* B **70** 214421
[14] Chattopadhyay M K, Roy S B and Chaddah P 2005 *Phys. Rev.* B **72** 180401(R)
[15] Roy S B *et al* 2004 *Phys. Rev. Lett.* **92** 147203 and the references therein
[16] Roy S B, Chattopadhyay M K, Chaddah P and Nigam A K 2005 *Phys. Rev.* B **71** 174413
[17] Imry Y and Wortis M 1979 *Phys. Rev.* B **19** 3580
[18] Chattopadhyay M K and Roy S B, unpublished results
[19] Chattopadhyay M K, Manekar M A and Roy S B 2006 *J. Phys. D: Appl. Phys.* **39** 1006